

Allogeneic adipose-derived stem cells regenerate bone in a critical-sized ulna segmental defect

Congji Wen^{1,2,*}, Hai Yan^{3,*}, Shibo Fu¹, Yunliang Qian¹, Danru Wang¹ and Chen Wang¹

¹Department of Plastic and Reconstructive Surgery, Shanghai 9th People's Hospital, Shanghai Jiao Tong University School of Medicine, 639 Zhi Zao Ju Road, Shanghai, 200011, People's Republic of China; ²Department of Plastic Surgery, Yancheng First Peoples' Hospital, 16 Yue He Road, People's Republic of China. 224000; ³Department of Orthopedics, Nantong Rich Hospital, No. 2000 Lake Avenue, Nantong, 226010, People's Republic of China

*Authors who contributed equally

Corresponding authors: Chen Wang. Email: wangchen2369@163.com; Danru Wang. Email: wangdanru@163.com

Abstract

Adipose-derived stem cells (ASCs) with multilineage potential can be induced into osteoblasts, adipocytes and chondrocytes. ASCs as seed cell are widely used in the field of tissue engineering, but most studies either use autologous cells as the source or an immunodeficient animal as the host. In our present study, we explored the feasibility of applying allogeneic ASCs and demineralized bone matrix (DBM) scaffolds for repairing tubular bone defects without using immunosuppressive therapy. Allogeneic ASCs were expanded and seeded on DBM scaffolds and induced to differentiate along the osteogenic lineage. Eight Sprague–Dawley (SD) rats were used in this study and bilateral critical-sized defects (8 mm) of the ulna were created and divided into two groups: with ASC-DBM constructs or DBM alone. The systemic immune response and the extent of bone healing were evaluated post-operatively. Twenty-four weeks after implantation, digital radiography (DR) testing showed that new bones had formed in the experimental group. By contrast, no bone tissue formation was observed in the control group. This study demonstrated that allogeneic ASCs could promote bone regeneration and repair tubular bone defects combined with DBM by histologically typical bone without systemic immune response

Keywords: Adipose-derived stem cells, allogeneic, ulna bone regeneration, ulna model, demineralized bone matrix

Experimental Biology and Medicine 2016; 241: 1401–1409. DOI: 10.1177/1535370215576298

Introduction

Repair of excessive bone defects caused by trauma, surgery or primary tumor resection pose a severe challenge to orthopedic surgery.¹ Autologous bone graft is regarded as the gold standard for treatment of these orthopedic problems. However, this method is limited by the availability of appropriate bone grafts, and patients may develop complications such as postoperative nonunion and donor-site morbidity, which influence the therapeutic efficacy of the treatment and reduce quality of life.¹ Many different graft materials have been used for autologous bone grafts in clinical applications to treat bone defects, and demineralized bone matrix (DBM) has proven to be effective for bone grafting procedures.^{2–4}

Bone tissue engineering techniques that seed cells onto scaffolds provide an optimal method for repairing large bone defects. The utilization of such techniques has shown great potential, especially in disunion fractures where endochondral ossification occurs during wound healing.⁵ DBM has been widely used in bone tissue engineering because of

its osteoinductive and osteoconductive features.⁶ DBM contains large quantities of bioactive substances which can stimulate the growth and fusion of grafted bone.⁷

To create viable bone tissue substitutes, live, metabolically active cells must be used to produce continuous scaffolds and repair large bone defects. Adipose-derived stem cells (ASCs) are multipotent stem cells that can differentiate into osteoblasts, adipocytes and chondrocytes. Recently, many researches have demonstrated that ASCs combined with various biocompatible-3D scaffolds could form homogeneous bone-like tissue.⁸

ASCs have many advantages and are commonly used to repair bone defects through autologous transplantation; however, isolating and expanding these cells before transplantation is a time-consuming process. *In vitro* studies demonstrate that ASCs do not stimulate incompatible lymphocyte reaction of allograft, and moreover, they actively inhibit mixed lymphocyte reactions (MLRs) and lymphocyte proliferative responses to mitogens.⁹ Recently, it has been reported that allogeneic ASCs can be successfully transplanted in conjunction with a natural coral

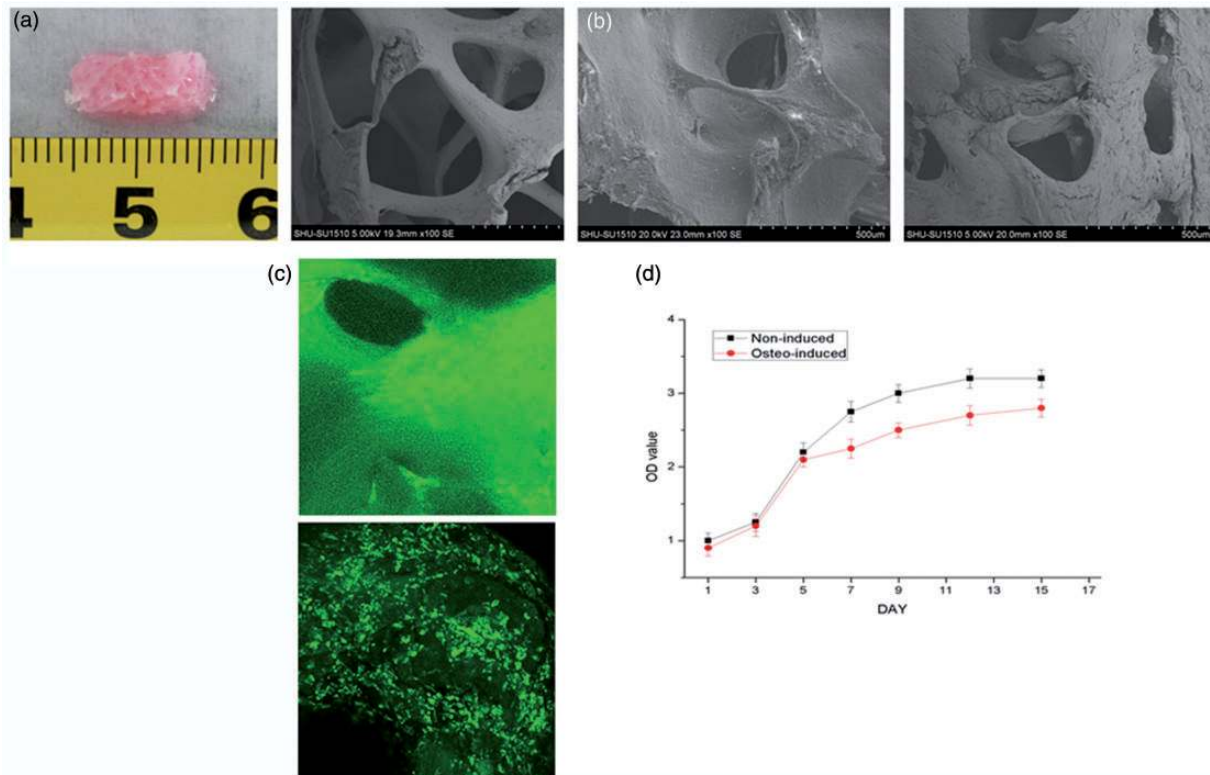


Figure 1 Attachment and growth of ASCs on the DBM scaffold. (a) Gross view (left panel; $3 \times 5 \times 8 \text{ mm}^3$) and SEM image (right panel; $\times 100$) of the DBM scaffold. (b) Matrix deposition by ASCs on the DBM scaffold after three and seven days (left and right panels, respectively) as determined by SEM. (c) Confocal analysis of DiO-labeled ASCs after three and seven days (top and bottom panels, respectively). (d) Proliferation of osteo-induced and non-induced ASCs on the DBM scaffold as determined by a DNA assay using Hoechst 33258 dye. Each OD value represents the mean of three independent experiments. (A color version of this figure is available in the online journal.)

scaffold to heal cranial critical-sized defects (CSD) in a canine model.¹⁰

The aim of our study was to evaluate repair outcomes of critical-size ulna defects in SD-rats by grafting an osteogenic scaffold that had been seeded with allogeneic ASCs. We hypothesized that this ASC/DBM would induce new bone formation and heal critical-size ulna defects successfully.

Materials and methods

Cell culture, scaffold seeding and osteogenic differentiation of ASCs

The Animal Care and Use Committee of Shanghai Jiaotong University of Medicine approved all animal experimental protocols. Allogeneic adipose tissue was isolated from the inguinal fat pad of adult SD-rats under inhaled anesthesia. Adipose tissue was minced and rinsed with phosphate-buffered saline (PBS). The extracellular matrix was digested with 0.1% (wt/vol) collagenase type I and shaken thoroughly at 37°C for 90 min. The growth medium (DMEM containing 10% FBS and 1% penicillin-streptomycin) were added to neutralize the enzyme. After 5-min centrifugation, the pellet was suspended in red blood cell lysis buffer and incubated for 10 min, then the tubes were centrifuged, and the supernatants were again discarded. The cell pellets were washed twice with PBS, and the cells were suspended in fresh growth medium. After 4–16 h of incubation,

the unattached cells were removed by washing with PBS. The remaining adherent cells were maintained at 37°C and 5% CO_2 and were considered to be ASCs. The medium was changed 24 h after seeding and every three days thereafter. Cells were passaged when the cultures reached 70% to 80% confluency. After the third passage (P3), subconfluent cells were trypsinized, and 3×10^5 cells were seeded onto a $3 \times 5 \times 8 \text{ mm}^3$ DBM scaffold. The cell suspension was slowly pipetted onto the scaffold using a 1000 ml pipette to draw the suspension bi-directionally three times. After incubation at 37°C for 4 h to allow the cells to attach to the scaffold, the ASC/DBM composites were cultured in osteogenic medium, and the medium was changed every three days. Cultures were osteogenically induced for 10–15 days and used for further study.

It has been proven that primarily cultured ASCs have the ability to grow into adipocytes, chondrocytes and osteoblasts.¹¹ Adipogenic differentiation, as indicated by the presence of Oil Red O-staining intracellular lipid droplets, was evaluated in our cultures. With the method of micromass culture, chondrogenic differentiation, characterized with type II collagen deposition, was examined by immunofluorescence staining. Osteogenic differentiation was revealed by the positive ALP staining and alizarin red staining.

SEM and porosity measurement of DBMs

DBMs were obtained from the National Tissue Engineering Center (Shanghai, China). They were prepared from

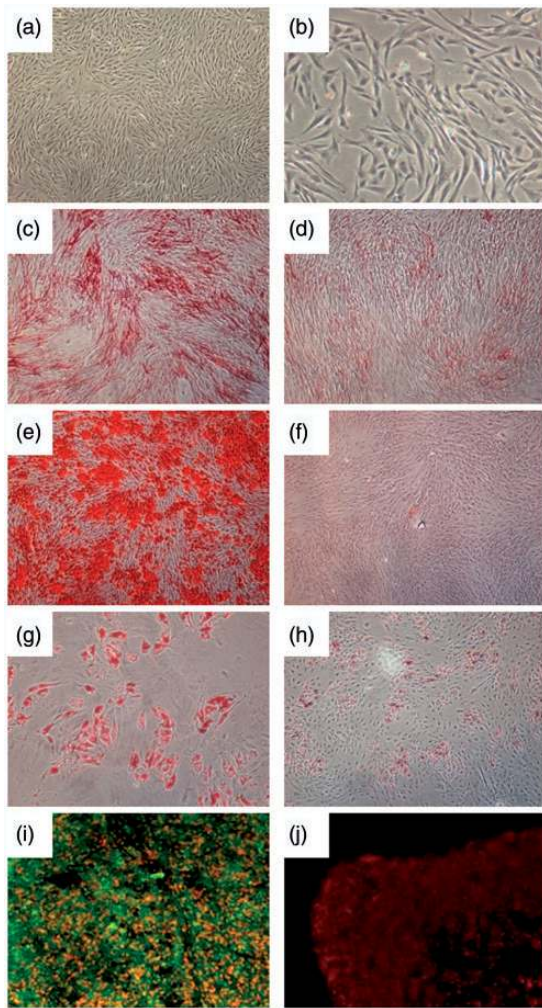


Figure 2 Morphology and multilineage differentiation of rat ASCs. (a, b) ASCs exhibited a fibroblast-like morphology as observed under a phase contrast microscope at passage 0 and 3, respectively. Osteogenic differentiation was revealed by the positive ALP staining (c) and alizarin red staining (e). Adipogenic differentiation was confirmed by positive Oil Red O staining (g). Chondrogenic differentiation was verified by immunofluorescence staining for the presence of collagen type II (i). Negative ALP staining, alizarin red staining, Oil Red O staining and collagen type II staining were also shown as well (d, f, h, j). (scale bars: 100 μm for a, c-f, h-j, and 50 μm for b and g). (A color version of this figure is available in the online journal.)

pig bone matrix in a process according to the method described by Gruskin et al.,⁷ and were trimmed to 3 mm \times 5 mm \times 8 mm and sterilized with ethylene oxide at 38°C before use. SEM was used to observe the morphology of the DBM scaffold. The scaffolds were gold-coated and viewed with XL-30 microscope to observe the surface and cross-sectional morphologies. The porosity of the scaffold was measured according to the literature.¹² Briefly, the freeze-dried scaffold was dehydrated by immersion in ethanol under vacuum for 20 min, and then taken out and weighed after absorbing the excess ethanol with filter paper. The porosity was calculated according to the following formula: $\text{porosity} = [(W1 - W2) / \rho V] \times 100\%$, where W1 and W2 represent the weights of the scaffold before and after immersion in ethanol, respectively, ρ is the density of ethanol and V is the volume of the scaffold.

Preparation of ASCs/DBM implants

ASCs at passage 3 were harvested and suspended in the osteogenic medium at a density of 1×10^7 cells/mL. Corresponding cells were slowly pipetted onto the DBM scaffold using a 2 mL pipetter to draw the suspension bidirectionally three times. After being incubated at 37°C for 4 h to allow cell attachment, the ASCs/DBM composites were cultured in 20 mL of osteogenic medium for a further 14 days before animal experiment with the medium exchanged every three days. DBM scaffolds without loading cells but cultured under the same condition for 14 days were used as controls.

To visualize the cell attachment and spatial distribution on the scaffold, Dio-labeled ASCs were subjected to the fluorescence microscope (Leica Microsystem, Germany) examination and scanning electron microscopy (Philips XL-30, Netherlands) detection at day 3 and day 7 after cell implantation.

By DNA assay, the proliferation of ASCs seeded in the DBM scaffolds was detected at days 1, 3, 5, 7, 9, 12, and 15 post-inoculation. In brief, the ASCs/DBM composites collected at different time points were ground completely for full lysis and cultured with proteinase K (Sigma) at 56°C overnight. Measure the fluorescence of each sample to quantify the DNA content using Hoechst 33258 dye (Sigma) by corresponding to a standard curve. The DNA standard curve was developed by lysing serial dilutions of rat ASCs with a known concentration. The osteogenic phenotype of ASCs was determined by alkaline phosphatase (ALP) activity and accumulated calcium assay at days 1, 4, 7, and 14 after cell seeding.

Surgical procedure

Eight healthy six-month-old adult SD-rats were included in this study. A 5-cm longitudinal incision in the middle portion of the ulna was made¹³ and dissection was performed carefully to minimize disruption of the musculature. A transverse osteotomy was created in the ulna midshaft. The fractured ulna was reduced and aligned, a disjuncting of 8 mm between bone fragments was performed, and the periosteum was exenterated near the fracture ends to guard against membranous bone formation. DBM with ASCs was then fixed into the left defect of the experimental group. DBM alone was transplanted around the fracture of the right ulna as control. Neither groups needed a fixture. Muscle and fascia were reapproximated and sutured, and the incision was closed in a routine fashion. From the next day and for the rest of the study period, all rats were allowed unrestricted activity in individual cages.

Detection of systemic immunological reactions

To detect systemic immunological reactions, 2 ml of blood was drawn from the jugular vein of each animal at selected time points post-operatively. The ratios of CD4-positive to CD8-positive lymphocytes (CD4/CD8) were evaluated by flow cytometry at post-operative days 0, 2, 4, 6, 8, 10, 12, and 14. The serum cytokine levels, including the levels of interleukin (IL)-2, IL-4, IL-10, interferon (IFN)- γ and transforming growth factor β 1 (TGF- β 1) were measured using ELISA

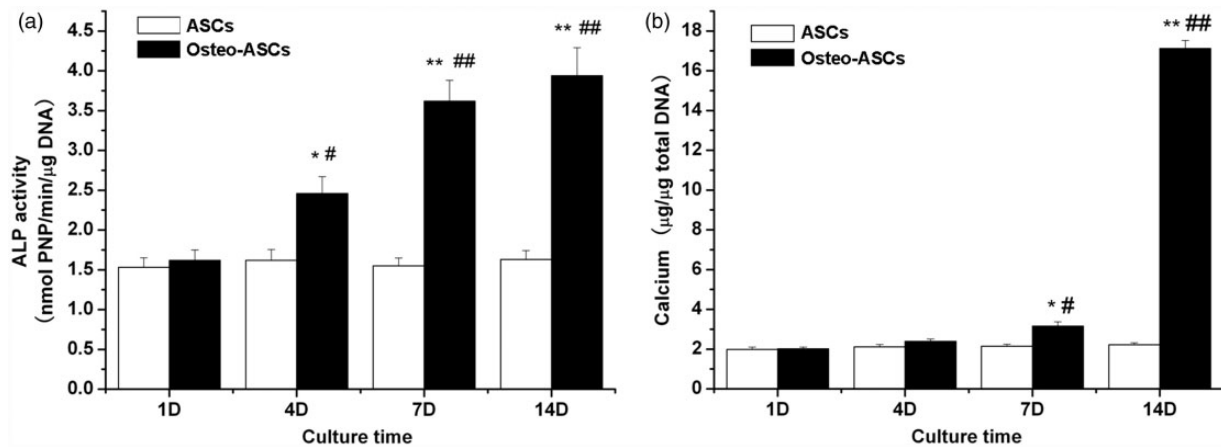


Figure 3 *In vitro* characterization of the osteogenic differentiation capacity of ASCs on the DBM scaffold. ASCs cultured on DBM scaffold was evaluated by the expression of ALP (a) and accumulated calcium (b) at days 1, 4, 7 and 14 post-seeding, respectively. DBM scaffold seeded with undifferentiated ASCs served as a control. * $P < 0.05$ vs respective undifferentiated ASCs controls, ** $P < 0.01$ vs undifferentiated ASCs controls, # $P < 0.05$ vs one-day osteo-differentiated ASCs cultured with OM, ## $P < 0.01$ vs one-day osteo-differentiated ASCs cultured with OM. OM: osteogenic medium

kits according to the manufacturer's protocols (Jiancheng Biotechnology Company, Nanjing, China) at postoperative weeks 0, 1, 2, 4, 12, and 24.

Radiographic examination

Animals were anesthetized and radiographs were performed at 24 weeks post-transplant to assess the repair result of the bone defects.

Histological examination

Tissues taken from the defect areas of both groups were marked post-implantation ($n = 4$). The samples were decalcified with a 10% EDTA solution for two weeks before they were dehydrated in a series of alcohol washes. Tissues were then embedded in paraffin, sectioned at a thickness of 5 μm and processed for routine hematoxylin and eosin (HE) staining.

Tensile tests

At post-operative week 24, four rats were killed and the ulnas were explanted. The surrounding soft tissues were removed from the ulna. The explanted ulnas were then assessed manually for tensile resistance using a tensile testing machine (Instron-4456, Norwood, MA, USA).¹⁴

Statistical analysis

All data are expressed as the mean \pm standard deviation (SD). Statistical analysis was performed by one-way ANOVA and paired Student's *t*-test using SPSS 11.0 software. A *p*-value of less than 0.05 was considered significantly different.

Results

Adherence and growth of ASCs on the DBM scaffold

In general, DBM is composed of three-dimensional porous structures of considerable mechanical strength.

In spite of different aperture diameters, it has suitable interval porosity and aperture size. Examination by scanning electron microscopy showed a loose material with relatively large apertures. All of the pores were interconnected and possessed a reticular porous structure with a mean pore diameter of $348.98 \pm 51.68 \mu\text{m}$ and a volume porosity of $87.87 \pm 1.55\%$ (Figure 1(a)). To prepare the ASC/DBM composites for transplantation, DBMs were trimmed into 3 mm \times 5 mm \times 8 mm cylinders that were the same size as the defect created in the SD-rat model.

In primary cultures, ASCs extracted from rat inguinal fat pads were a relatively homogenous population and exhibited typical fibroblast-like morphological characteristics with a fusiform shape (Figure 2(a) and (b)). After incubation of ASCs in osteogenic medium, osteogenic differentiation of ASCs was observed by positive expression of ALP (Figure 2(c)) and calcium deposition (Figure 2(e)). Adipogenic differentiation was detected by detecting red lipid droplets throughout the cytoplasm by Oil Red O staining (Figure 2(g)). Chondrogenic induction of ASCs was confirmed by characteristic deposition of collagen type II with immunofluorescence staining (Figure 2(i)).

After sufficient incubation in osteogenic medium, SEM observation manifested that ASCs adhered well to the scaffold at day 3 post-inoculation. Most ASCs presented a sharp elongated spindle morphology at day 7 post-inoculation, and the seeded cells spread in a determined direction and formed a confluent layer of ASCs covering the surface of scaffolds (Figure 1(b)). In addition, the cells deposited in the pores secreted a large amount of extracellular matrix. The clusters of cells were distributed evenly across the DBM scaffold. To examine the growth and distribution of ASCs on DBM, fluorescent DIO-labeled cells were detected with a confocal fluorescence microscope. After three days seeded on the scaffold, cells were relatively evenly distributed on the surface of the scaffold with a low density. At day 7, a high density cells filled most of apertures of the scaffold

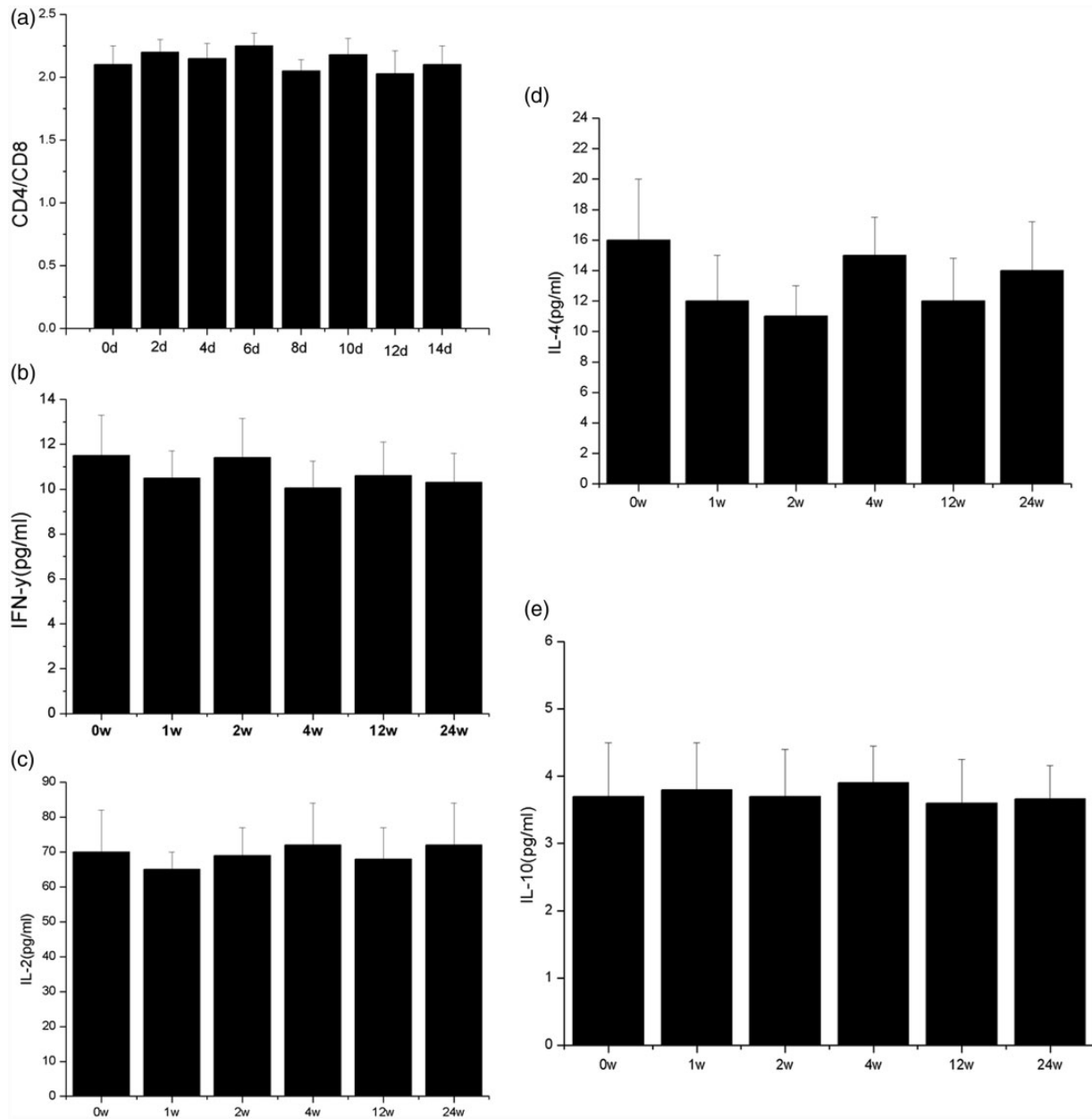


Figure 4 Systemic immunological reactions after allogeneic ASC/DBM transplantation. (a) Flow cytometric analysis revealed no significant changes in CD4/CD8 ratios at postoperative days 2, 4, 6, 8, 10, 12 and 14, compared with that of day 0 ($n=8$). (b–e) No changes in serum IFN- γ (b), IL-2 (c), IL-4 (d), and IL-10 (e) were detected at postoperative weeks 0, 1, 2, 4, 12 and 24, compared to the corresponding values on week 0 ($n=8$). Data represent the mean of three independent experiments performed at each time point

with green fluorescence labeled (Figure 1(c)). The Hoechst 33258 assay showed that the proliferative ability of cells cultivated on DBM was no less than those grown on culture dishes, suggesting that the DBM is biocompatible with ASCs (Figure 1(d)).

Osteogenic differentiation of ASCs on the DBM scaffold

To further certify whether the ASCs seeded on the DBM scaffold could maintain the characteristic of ossification, the expression of ALP and the accumulated calcium were measured on days 1, 4, 7, and 14 after seeding,

respectively. In Figure 3(a), the expression of ALP in the osteo-differentiated group began to increase by day 4, and continued through days 7 and 14. Accumulated calcium by osteo-differentiated ASCs increased slightly by day 7, and increased significantly by day 14 (Figure 3(b)). Both ALP expression and accumulated calcium in the undifferentiated group remained at a relatively constant low levels throughout the testing. Significantly elevated ALP activity was observed in the osteo-differentiated group at each time point tested from day 4 ($P < 0.05$) on, whereas accumulated calcium activity was observed in the osteo-differentiated group from

day 7 ($P < 0.05$) onward, compared to the undifferentiated ASCs. Because the expression of ALP and accumulated calcium were synergistically increased at day 14, cells/DBM composites should be cultured for 14 days *in vitro* before *in vivo* implantation.



Figure 5 Ulna bone repair at 24 weeks post-implantation. The defect was repaired at 24 weeks after surgery in ASC/DBM-treated animals (left panel) but not after treatment with DBM alone (right side). The DBM was almost completely degraded

Detection of systemic immunological reactions

All of the animals recovered from the surgical procedure rapidly, without complications. During the observation period, none of the rats displayed fever, infection, swelling, implantation site dehiscence or abnormal craniofacial or cervical lymph nodes. CD4/CD8 cell ratios were determined using flow cytometry at post-operative days 0 (baseline), 2, 4, 6, 8, 10, 12 and 14. The values showed a slight but not significant increase at days 4 and 14 compared with day 0. At other time points, smaller (but not significant) changes were found ($P > 0.05$, Figure 4(a)). The serum concentrations of IL-2, IL-4, IL-10, IFN- γ and TGF- β 1 were also measured at post-operative weeks 1, 2, 4, 12 and 24. No significant differences were detected compared to the corresponding values on week 0 ($P > 0.05$, Figure 4(b)–(e)).

Radiographic examination

To evaluate engineered ulnar bone repair, radiographs were taken at 24 weeks post-implantation. Ulnas implanted with ASC/DBM constructs demonstrated that both in the areas immediately adjacent to the host bone and within the central region of the implant, the volume and radiopacity of newly formed bone was highly increased, and the bone

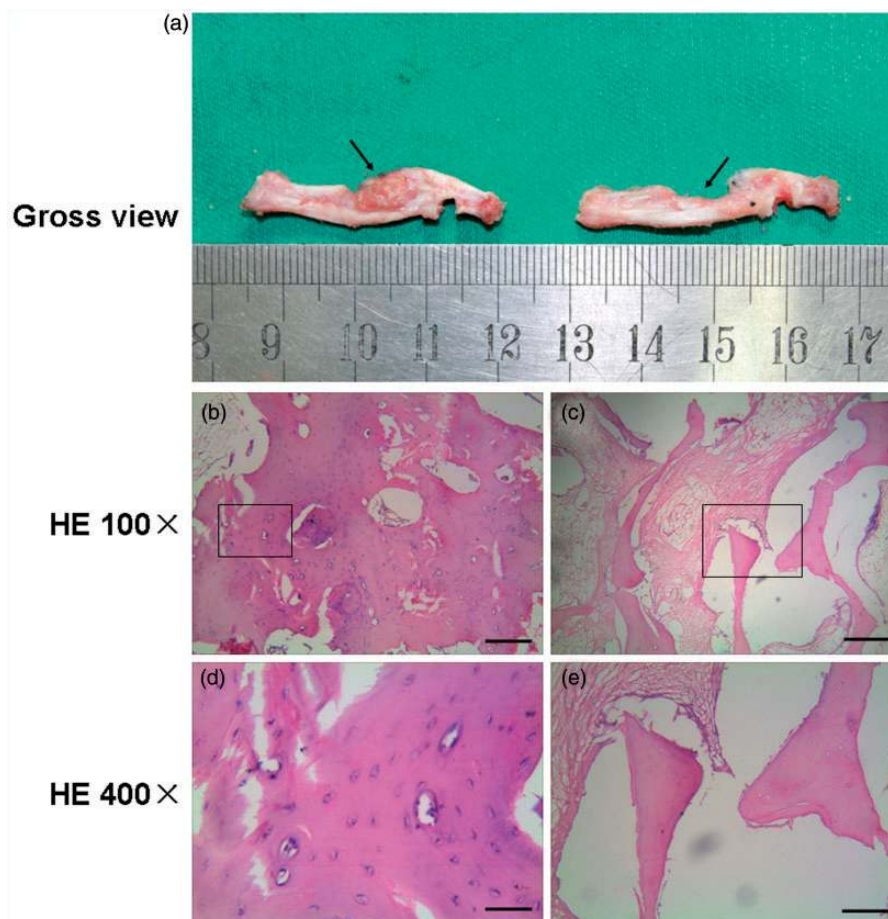


Figure 6 Analysis of the repaired ulna bone defects. (a) Gross view showed that ulnar bone defect was healed in either allogeneic ASCs (left panel) or DBM-alone treated sites (right panel) (arrows indicate locations of the ulnar bone defects). (b–e) HE staining revealed the mature bone structure within the cell/scaffold treated defects at 24 weeks, while the DBM alone treated defect was filled with loose fibrous tissue at $\times 100$ (b and d, scale bar: $100\ \mu\text{m}$) and $\times 400$ (c and e, scale bar: $50\ \mu\text{m}$) ($n = 4$). (A color version of this figure is available in the online journal.)

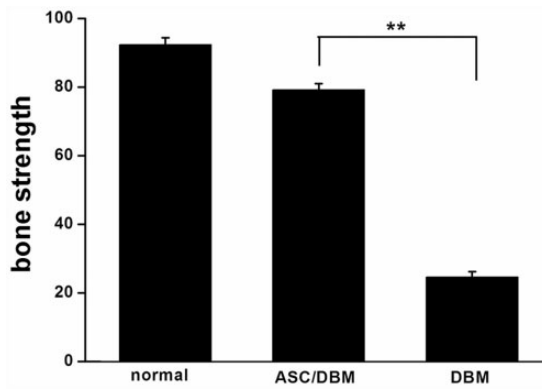


Figure 7 Effects of ASC/DBM transplantation on tensile strength. Tensile tests were conducted at 24 weeks after surgery. Data represent mean of three independent experiments for each animal ($n = 4$). $**P < 0.01$ compared with groups with DBM alone

contour was remodeled smoothly (Figure 5). Conversely, in the control slides, no obvious consistent callus extended over the gaps, and radiolucency at the cutting ends was observed.

Gross view and histological examination

Compared with radiographic analyses, gross view and histological examination of the repaired tissue were more intuitive. At 24 weeks post-implantation, a new bone was observed at the bony margin of the defect (Figure 6(a)), the gross view of ulnar bone showed that the experimental side resembled that of normal ulnar bone, whereas the defect of control side was full of fibrous-like tissue.

Histological examination revealed a defect completely closed with new bone that consisted of marrow spaces and a more mature trabecular bone (Figure 6(b) and (c)). There were an increased number of lacunar cells and osteocytes with the normal structure of mature bone in the regenerated bone. In contrast, in the control defect, no osteogenesis was observed, only fibrous tissue and residual DBM were present (Figure 6(d) to (e)).

Tensile tests

To evaluate the mechanical properties of the reconstructed ulna, tensile tests were performed at 24 weeks after surgery. In ASC/DBM groups, the bone strength of the regenerated bone was lower than that of the contralateral normal ulna. However, there were significant differences ($P < 0.05$, Figure 7) in tensile strength compared to the control groups with DBM only.

Discussion

Treating excessive bone defects remains a major challenge to orthopedic surgeons. It has been demonstrated that the use of autologous bone segmental transplants may simultaneously provide vascularity and structural support with good success rates.² However, this method is time consuming and is associated with several complications, including thrombosis of the anastomosed vessels, stress fractures,

infection and variable donor-site morbidity.² Along with the development of medications, the use of alternative substances to autologous bone is promising for such treatment. Stem cells such as BMSCs or ASCs, as well as growth factors, such as platelet-derived growth factor (PDGF) and bone morphogenetic proteins (BMPs),¹⁵ and scaffolds are useful for restoring critical-size bone defects.¹⁶ Nonetheless, only one of the above options is clearly inadequate. ASCs have been extensively proven to have good osteogenic capacity both *in vitro* and *in vivo*,¹⁷ and ASCs are abundant in adipose tissue, which is available in large quantities under local anesthesia.⁵ However, it is time-consuming to isolate and expand these cells before autologous transplantation, so prepared allogeneic ASCs maybe a good alternative source for use in an emergency. Because of the intrinsic immunogenicity of osteoblasts, which express MHC I and II together with some other co-stimulatory molecules such as CD80, CD86 and CD54, there is a strong alloreactive immune response when transplanting bone allograft into a host.¹⁸ Surprisingly, ASCs have been reported not to express MHC I, MHC II and the costimulatory molecules CD80 (B7-1), CD86 (B7-2) and CD40, and to display low immunogenicity and negative immunomodulation *in vitro*.¹⁹ Liu et al. reported that allogeneic ASCs could heal cranial critical-sized defects without the use of immunosuppressive therapy.¹⁰ The goal of our research remains to study the potential therapeutic effects of allogeneic ASCs in the treatment of critical-size rat ulnar defects using a tissue-engineering approach.

As mentioned before, ASCs display the properties of low immunogenicity and negative immunomodulation, and it has been found that ASCs keep these 'immunoprivileged' properties when differentiating into osteoblasts *in vitro*.¹⁹ In our study, at one week post-implantation, all wounds were healed by first intention, without hematoma and extravasate. At 24 weeks post-implantation, there was no significant systemic immune response, and no necrosis, suppuration or fluid within the implant or surrounding bone. In addition, the soft tissue had bonded to the scaffold without capsule formation, indicating that allogeneic osteo-differentiated ASCs are acceptable to host animals in the ulna defect model studied here. These results confirmed again that allogeneic ASC implants contribute directly to bone regeneration. In addition, ASCs could serve as a good option of cell source for bone repair in clinical use.

A prerequisite for any tissue engineering approach is that the control defects heal more slowly than the experimental defects. A critical size defect is defined as the smallest intraosseous wound that cannot heal by bone formation during the lifetime of the animal.¹³ Relatively, small defects were able to undergo self-repair with endogenous progenitor cells and differentiation factors. Dudaset et al. used osteo-induced ASCs seeded onto gelatin foam (GF) scaffolds to repair noncritical-sized calvarial defects²⁰; however, the ASC treatment groups did not exhibit greater healing than the untreated defects. One possible reason is that the designed defects used in the experimental group were considerably smaller than critical-sized defects.¹³ However, in critical-sized defects, when the bone repair scaffold is implanted alone, either the number or migration rate of

normal osseous cells around the defect cannot meet the conditions for regenerating the new bone before the degradation of the scaffold, resulting in fibrous-like tissue at the defect. In this study, defects treated with the scaffold alone had a lower elastic stiffness, and no osseous union could be formed except a little osseous tissue formation found at the cutting edge of normal osseous tissue. ASCs appear to promote bone growth. The repair in animals that received the scaffold with ASCs showed significantly more bridging callus than the scaffold-alone repairs. It is worth mentioning that seeded ASCs, in addition to providing an osteogenic cell source for new bone formation, may secrete certain growth factors to recruit native cells to the defect site. However, no evidence supporting this mechanism has yet been found.

A suitable scaffold for bone regeneration must be biocompatible with the host to allow cell attachment, proliferation, ECM deposition, and to provide skeletal support for *in vivo* bone regeneration.²¹ DBM plays a pivotal role in our research and can provide a substrate for bone formation and allow angiogenesis to occur.^{22–24} In addition, DBM contains osteo-inductive factors which stimulates the filling of gaps and defects with new bone.¹⁴ When transplanted into the defect, DBM acts as a scaffold for the ingrowth of vessels, followed by resorption of the implant and deposition of new bone derived from the edges of the defect.⁷ At present, DBM is a commonly clinically used bone graft substitute with success in repairing bone defects. The porous structure of DBM makes it a satisfied biomaterial for bone tissue engineering. In this study, ASCs were osteo-induced as early as passage 3, seeded onto scaffold and cultured *in vitro* for 10–15 days before transplanted into the defect. It is speculated that the growth speed of ASCs osteo-induced in the presence of DBM may be greater than that of cultures osteo-induced in a two-dimensional tissue culture flask. We also found expression of osteogenesis-related active proteins such as ALP and extracellular Ca²⁺ by *in vitro*-cultured ASCs with no osteo-induction, which indirectly demonstrates that DBM can induce ASCs to produce osteoblasts.

LF et al. reported that the hMSC (human mesenchymal stem cell)/scaffold had a significantly higher elastic and viscous stiffness and higher phase angles than scaffold alone when treating critical-sized defects.²⁵ Our study also indicate that application of ASCs on scaffolds significantly enhances the biomechanical properties of ulnar repair for critical segmental defects. At 24 weeks after surgery, the bone strength of the regenerated bone was obviously higher in ASC/DBM groups than that of the control groups. Mechanical properties are believed to be connected with the architecture of bone, and different bone structure leads to different tensile strengths. In the present study, the histological observation score corresponded favorably with tensile tests. At 24 weeks post-surgery, there were many lacunar cells and osteocytes with the normal structure of mature bone in the ASC/DBM sides. In contrast, no osteogenesis could be found, except fibrous tissue and residual DBM at the control defect. Thus ASCs, upon differentiation, may follow a pathway similar to that of osteoblasts in bone turnover. In the current study, we found that allogeneic

osteodifferentiated ASCs combined with DBM scaffolds could regenerate bone in a rat ulna critical-sized defect model, attaining bone healing with sufficiently high bone density and adequate bone tensile strength. Further studies are needed to compare our results to defects repaired by autologous osteodifferentiated ASCs or different scaffolds.

Authors' Contributions: CW, ChW, and DW conceived and designed the experiments, YC and YZ performed the experiments, HY and YQ analyzed the data, SBF contributed reagents/materials/analysis tools, CW ChW wrote the paper, and CW and HY contributed equally to this work.

ACKNOWLEDGEMENTS

This work was financially supported by the National Natural Science Foundation of China (grant no 81201204).

DECLARATION OF CONFLICTING INTERESTS

The author(s) declared no potential conflicts of interest with respect to the research, authorship, and/or publication of this article.

REFERENCES

- Porter JR, Ruckh TT, Popat KC. Bone tissue engineering: a review in bone biomimetics and drug delivery strategies. *Biotechnol Prog* 2009;**25**:1539–60
- Petri M, Namazian A, Wilke F, Ettinger M, Stübig T, Brand S, Bengel F, Krettek C, Berding G, Jagodzinski M. Repair of segmental long-bone defects by stem cell concentrate augmented scaffolds: a clinical and positron emission tomography-computed tomography analysis. *Int Orthop* 2013;**37**:2231–37
- Beris AE, Lykissas MG, Korompilias AV, Vekris MD, Mitsionis GI, Malizos KN, Soucacos PN. Vascularized fibula transfer for lower limb reconstruction. *Microsurgery* 2011;**31**:205–11
- Meyle J, Hoffmann T, Topoll H, Heinz B, Al-Machot E, Jervøe-Storm PM, Meiss C, Eickholz P, Jepsen S. A multi-centre randomized controlled clinical trial on the treatment of intra-bony defects with enamel matrix derivatives/synthetic bone graft or enamel matrix derivatives alone: results after 12 months. *J Clin Periodontol* 2011;**38**:652–60
- Rodriguez AM, Elabd C, Amri EZ, Ailhaud G, Dani C. The human adipose tissue is a source of multipotent stem cells. *Biochimie* 2005;**87**:125–8
- De Long WG Jr, Einhorn TA, Koval K, McKee M, Smith W, Sanders R, Watson T. Bone grafts and bone graft substitutes in orthopaedic trauma surgery. A critical analysis. *J Bone Joint Surg Am* 2007;**89**:649–58
- Gruskin E, Doll BA, Futrell FW, Schmitz JP, Hollinger JO. Demineralized bone matrix in bone repair: history and use. *Adv Drug Deliv Rev* 2012;**64**:1063–77
- Seong JM, Kim BC, Park JH, Kwon IK, Mantalaris A, Hwang YS. Stem cells in bone tissue engineering. *Biomed Mater* 2010;**5**:062001
- Puissant B, Barreau C, Bourin P, Clavel C, Corre J, Bousquet C, Taureau C, Cousin B, Abbal M, Laharrague P, Penicaud L, Casteilla L, Blancher A. Immunomodulatory effect of human adipose tissue-derived adult stem cells: comparison with bone marrow mesenchymal stem cells. *Br J Haematol* 2005;**129**:118–29
- Liu GP, Zhang Y, Liu B, Sun J, Liu W, Cui L. Bone regeneration in a canine cranial model using allogeneic adipose derived stem cells and coral scaffold. *Biomaterials* 2013;**34**:2655–64
- Zuk PA, Zhu M, Mizuno H, Huang J, Futrell JW, Katz AJ, Benhaim P, Lorenz HP, Hedrick MH. Multilineage cells from human adipose tissue: implications for cell-based therapies. *Tissue Eng* 2001;**7**:211–28

12. Tian M, Yang Z, Kuwahara K, Nimni ME, Wan C, Han B. Delivery of demineralized bone matrix powder using thermogelling chitosan carrier. *Acta Biomater* 2012;**8**:753–62
13. Hollinger JO, Kleinschmidt JC. The critical size defect as an experimental model to test bone repair materials. *J Craniofac Surg* 1990;**1**:60–8
14. Iwasaki K, Kojima K, Kodama S, Paz AC, Chambers M, Umezu M, Vacanti CA. Bioengineered three-layered robust and elastic artery using hemodynamically equivalent pulsatile bioreactor. *Circulation* 2008;**118**:S52–7
15. Park SY, Kim KH, Shin SY, Koo KT, Lee YM, Seol YJ. Dual delivery of rhPDGF-BB and bone marrow mesenchymal stromal cells expressing the BMP2 gene enhance bone formation in a critical-sized defect model. *Tissue Eng Part A* 2013;**19**:2495–505
16. Feighan JE, Davy D, Prewett AB, Stevenson S. Induction of bone by a demineralized bone matrix gel: a study in a rat femoral defect model. *J Orthop Res* 1995;**13**:881–91
17. Amini AR, Laurencin CT, Nukavarapu SP. Bone tissue engineering: recent advances and challenges. *Crit Rev Biomed Eng* 2012;**40**:363–408
18. Shegarfi H, Reikeras O. Review article: Bone transplantation and immune response. *J Orthop Surg* 2009;**17**:206–11
19. Ren ML, Peng W, Yang ZL, Sun XJ, Zhang SC, Wang ZG, Zhang B. Allogeneic adipose-derived stem cells with low immunogenicity constructing tissue-engineered bone for repairing bone defects in pigs. *Cell Transplant* 2012;**21**:2711–21
20. Dudas JR, Marra KG, Cooper GM, Penascino VM, Mooney MP, Jiang S, Rubin JP, Losee JE. The osteogenic potential of adipose-derived stem cells for the repair of rabbit calvarial defects. *Ann Plast Surg* 2006;**56**:543–8
21. Cui L, Liu B, Liu G, Zhang W, Cen L, Sun J, Yin S, Liu W, Cao Y. Repair of cranial bone defects with adipose derived stem cells and coral scaffold in a canine model. *Biomaterials* 2007;**28**:5477–86
22. Hansen A, Pruss A, Gollnick K, Bochenin B, Denner K, Von Versen R, Hansen A. Demineralized bone matrix-stimulated bone regeneration in rats enhanced by an angiogenic dipeptide derivative. *Cell Tissue Bank* 2001;**2**:69–75
23. Rabie AB. Vascular endothelial growth pattern during demineralized bone matrix induced osteogenesis. *Connect Tissue Res* 1997;**36**:337–45
24. Zamboni G, Grano M. Biomaterials in orthopaedic surgery: effects of different hydroxyapatites and demineralized bone matrix on proliferation rate and bone matrix synthesis by human osteoblasts. *Biomaterials* 1995;**16**:397–402
25. Amorosa LF, Lee CH, Aydemir AB, Nizami S, Hsu A, Patel NR, Gardner TR, Navalgund A, Kim DG, Park SH, Mao JJ, Lee FY. Physiologic load-bearing characteristics of autografts, allografts, and polymer-based scaffolds in a critical sized segmental defect of long bone: an experimental study. *Int J Nanomedicine* 2013;**8**:1637–43

(Received July 26, 2014, Accepted January 28, 2015)